

CONCISE ARTICLE

[View Article Online](#)
[View Journal](#) | [View Issue](#)**Dual mode of action of phenyl-pyrazole-phenyl (6-5-6 system)-based PPI inhibitors: alpha-helix backbone *versus* alpha-helix binding epitope†**

Cite this: *Med. Chem. Commun.*, 2013, **4**, 1597

Natalya I. Vasilevich,* Ilya I. Afanasyev, Eugene A. Rastorguev, Dmitry V. Genis and Valery S. Kochubey

A new class of alpha-helix mimetics, based on the phenyl-pyrazole-phenyl (6-5-6) system, has been designed and synthesized. The ability of the new compounds to inhibit PPIs was confirmed using an MDM2-p53 binding assay. The library, containing completely new compounds, revealed an excellent hit rate of 15%, had satisfactory physicochemical properties (~38% soluble compounds), and the ligand efficiency of the best compound was 0.21 (0.22 for nutlin-3 in the same assay). Dual mode of action of these inhibitors was suggested based on computer modeling: depending on the nature of their substituents they could act as either an alpha-helix backbone mimetic or an alpha-helix binding epitope mimetic.

Received 24th July 2013
Accepted 20th September 2013

DOI: 10.1039/c3md00211j

www.rsc.org/medchemcomm

Protein–protein interactions are involved in regulating a variety of important cellular pathways *inter alia* in cancer development. Therefore they represent a highly attractive class of targets for drug discovery, which for a long time were considered as untreatable. However, essential progress has been made in recent years, and potent PPI inhibitors such as nutlin-3 and ABT-737 have been developed.^{1–6} It has been suggested that although protein interfaces are large, often a small subset of the residues (so-called “hot spots”) contributes significantly to the free energy of binding.⁷ These residues can be identified, for example, by alanine scanning mutagenesis. Analysis of the occurrence of hot spot amino acids in helix-mediated protein interfaces revealed that in most cases they are aromatic tyrosine, phenylalanine and tryptophan, or leucine and arginine.⁷ Secondly, it was found that the regions in the protein involved in the interactions are often organized in alpha-helices which deliver side chains to defined positions. This means that in order to get small molecule inhibitors, aromatic and hydrophobic groups which mimic the residues mentioned above should be placed in well-defined positions, and their relative orientation should be similar to those of the corresponding amino acid substituents in the alpha-helix region. Since most of the “hot spot” residues are located on the one recognition face (60% of all interactions⁷) these sites should correspond to the i, i+4 (i+3) and i+7 residues. As an example of such an approach, Fry and coworkers analyzed an alpha-helix epitope and generated a pharmacophore model for the mutual orientation of suitable hydrophobic groups.⁸

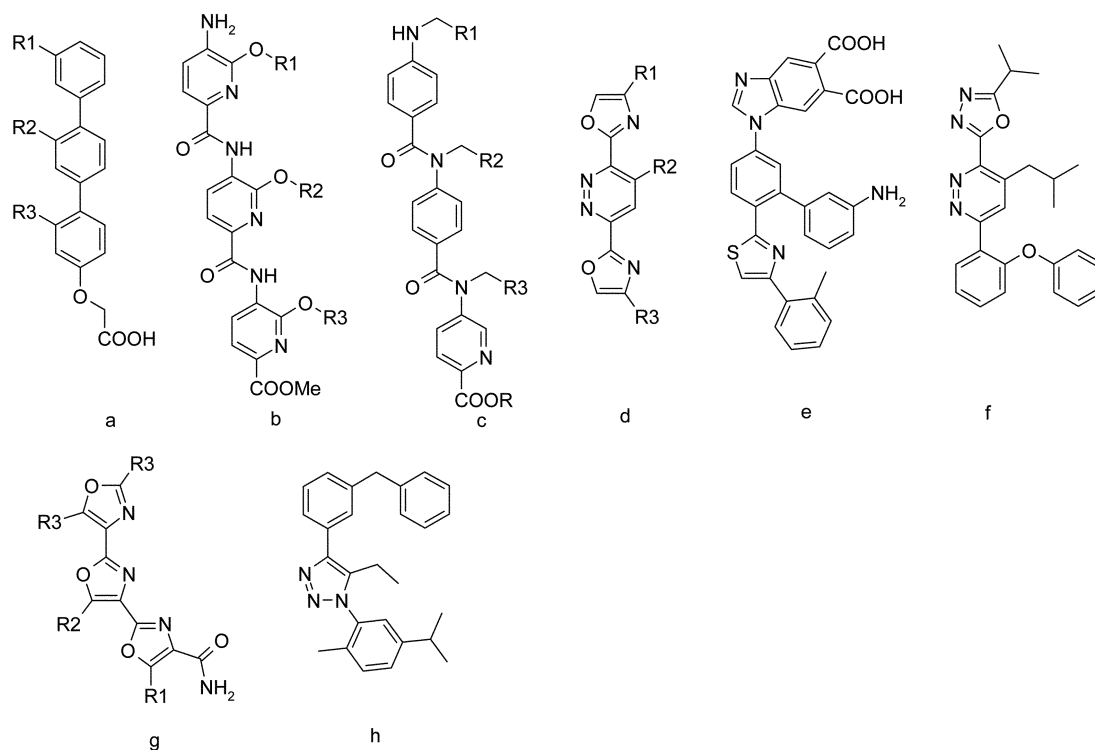
In the design of small molecule antagonists capable of interrupting protein–protein interactions, two approaches are generally employed: alpha-helix backbone mimetics and alpha-helix binding epitope mimetics (mimetics of both types are exemplified in Fig. 1). Both of these approaches have proved to be successful. The difference between them is that while the first approach includes the design of scaffolds which mimic alpha-helix backbones, and the side substituents occupy positions corresponding to the “hot spots”, the second approach does not utilize alpha-helix backbones but uses any core (often any heterocycle) which can place hydrophobic substituents in the appropriate positions. Both models have their inherent drawbacks: difficult and multi-step synthesis for the first model and deviation in side chain vector orientation from the vector in natural alpha-helices for the second model. Both groups tend to have poor solubility and absorption, distribution, metabolism and excretion (ADME) properties, requiring the incorporation of solubilizing groups.

However, sometimes assigning a scaffold to one of these types is not so obvious. In particular, this is relevant to the scaffolds containing five-membered heterocycles in the central position, as for scaffolds **g**⁹ and **h**¹⁰ (Fig. 1). In accordance with the reported calculations and crystallographic data, these scaffolds can adopt a conformation that mimics the alpha-helix backbone. On the other hand, the presence of the central five-membered ring makes the molecule slightly bent, and the core of compound **h** clearly resembles the core of the classical epitope mimetic nutlin. However, in contrast to nutlin, the central heterocycle in **h** is fully aromatic and does not allow any translatory motion, only rotation. Unfortunately there is no data about the biological activity of scaffolds **g** and **h** against PPI targets in the literature.

ASINEX Ltd., 20 Geroev Panfilovtsev Str., Moscow 125480, Russia

† Electronic supplementary information (ESI) available. See DOI: 10.1039/c3md00211j

Alpha-helix backbone mimetics



Alpha-helix binding epitope mimetics

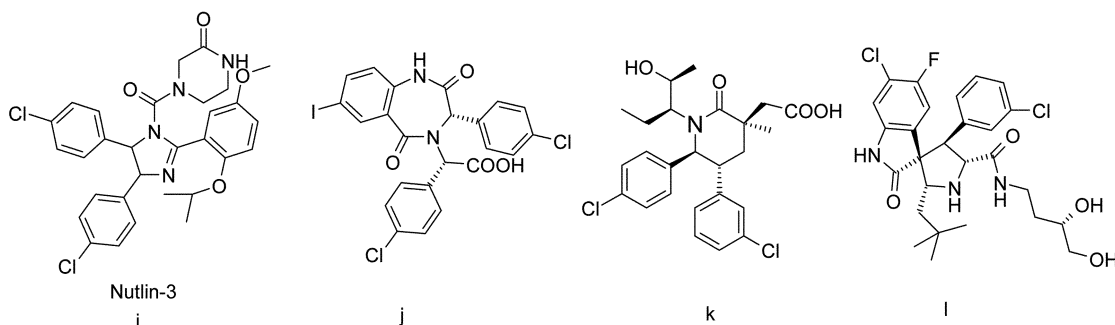


Fig. 1 Examples of the two types of small molecule antagonists of PPIs: α -helix backbone mimetics and α -helix epitope binding mimetics.

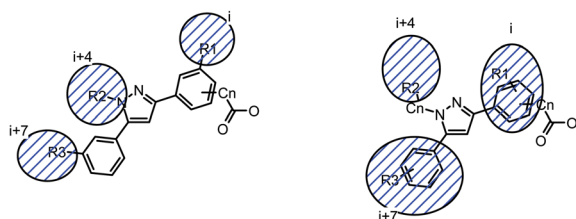


Fig. 2 Two modes of interaction assumed for compounds of the new scaffold with i, i+4 and i+7 subpockets.

In the present report we suggest a novel scaffold containing a five-membered heterocycle in the central position, which we assume to be able to serve as both an alpha-helix backbone

mimetic and an alpha-helix binding epitope mimetic, depending on the nature of the substituents (Fig. 2).

We suppose that when the R_1 and R_3 groups are large and hydrophobic, this scaffold acts as an alpha-helix mimetic and the phenyl-pyrazole-phenyl core mimics the alpha-helix backbone, and when the R_1 and R_3 groups are quite small, the scaffold acts as an epitope mimetic and both the terminal phenyl groups occupy subpockets corresponding to the side chains of the I and i+7 residues in the α -helix.

In addition, a carboxy group connected to one of the phenyl rings, directly or through a C_n linker, was introduced. This carboxy group can extend the value of our scaffold for several reasons. Firstly, it can serve as a solubilizing group. Secondly, the carboxy group is known to be over-represented among PPI

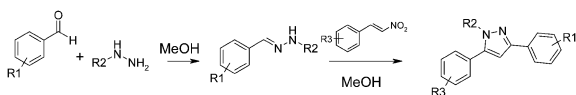
ligands,¹¹ so this group might potentially participate in additional interactions with the target. Finally, in accordance with our computer modeling, the carboxy group can serve as a synthetic handler which allows the introduction of an additional group corresponding to i+11 residues.

We elaborated a very feasible and straightforward “one pot” synthetic procedure, resulting in the creation of a library in a timely and cost effective manner. As a central ring, the pyrazole moiety was chosen as it is an important fragment in medicinal chemistry. It is well known that the synthesis of substituted pyrazoles is prone to result in a mixture of regioisomers. However, a method was published recently which describes the synthesis of pyrazoles from *N*-arylhydrazones and nitroolefins in a high yield and with excellent regioselectivity.^{12,13} We applied this new method to the synthesis of a medium-size library of 52 compounds (Scheme 1). A solution of hydrazine salt in methanol was added to an equimolar amount of aldehyde in methanol. After stirring at room temperature for 1 h, a solution of β -nitrostyrene (0.9 eq.) in methanol was added and the reaction mixture was stirred at room temperature for an additional 24 h, followed by chromatographic purification of the final product. It is worth mentioning that using di-substituted nitroolefins instead of nitrostyrenes allows the introduction of a fourth substituent to the pyrazole ring, which can be used for example as an additional solubilizing group (data not shown).

More than 80% of the compounds obtained meet the descriptor requirements which are favorable for PPI inhibitors such as SHP2, Mor11m, dipole, RDF070m, and Ui, suggested in the literature^{14–16} (see ESI†) and show satisfactory solubility in PBS buffer (38% of the compounds possess kinetic solubility $>0.2 \mu\text{M ml}^{-1}$). The molecular weights of the compounds were within the range of 373 to 597 Da.

As a model of protein–protein interactions, the MDM2-p53 interaction was chosen. All of the synthesized compounds were tested in the MDM2-p53 binding assay using a commercially available truncated p53 (17–26) containing the p53 binding domain. Truncation to residues 17–26 increases the affinity to MDM2 13-fold compared with the wild-type p53 peptide.¹⁷ As a consequence, the IC_{50} of nutlin-3, used as a reference in our assay, appeared to be 474 nM instead of 90 nM quoted in the literature.¹⁵ The results of the biological testing are given in Table 1, in comparison with nutlin-3.

It was found that 8 compounds possess an IC_{50} of less than $30 \mu\text{M}$, so the designed library possesses a relatively high hit rate of 15%. The ligand efficiencies for these compounds ranges from 0.12 to 0.21, so they are comparable with the ligand efficiency of nutlin-3 in our assay (0.22), and are very good for the library targeted on PPIs.^{1,18}



Scheme 1 Synthetic scheme for the preparation of phenyl-pyrazole-phenyl-based compounds.

Looking at Table 1, one can see that the most active compounds contain carboxylic groups directly linked to the phenyl ring, and elongation of the linker to CH_2COOH leads to ten-fold less active compounds (compare **1** and **18**, and **2** and **19**). Among the two tested *N*-pyrazole substituents (R^2), the longer and more flexible phenethyl group is better than the benzyl group. The phenyl-pyrazole-phenyl-based compounds appeared to be quite sensitive to R^3 substituents; while the methoxy derivative **34** possessed an IC_{50} of $185 \mu\text{M}$, the more lipophilic ethoxy (**4**), propoxy (**1**), butoxy (**5**) and isobutoxy (**2**) derivatives were among the most active compounds.

To prove our hypothesis about the possibility of a dual mode of interaction with MDM2, a docking study of two active compounds (**8** and **13**) into the MDM2 binding site of the MDM2 complex with p53 (PDB entry 1ycr) was performed. These compounds were chosen because they contain the smallest (**8**) and the bulkiest (**13**) R^3 substituents in the library, and therefore may adopt either alpha-helix backbone-like or nutlin-like modes of action. As is seen in Fig. 3, we found that depending on their substituents, these compounds (in yellow) may act either as alpha-helix backbone mimetics (left pane, in comparison with p53, in purple) or alpha-helix binding epitope mimetics (right pane, in comparison with nutlin-2). It is very interesting that in both cases, the compounds were docked into complexes with the transactivation domain of p53, but in the first case the optimal conformation seems to be alpha-helix-like, while in the latter case it is obviously nutlin-like.

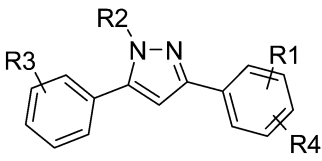
The compounds from our library were also partially tested against a Bcl-xl target, and some of them showed activity in the $120\text{--}600 \mu\text{M}$ range (data not shown), which could confirm the possible optimization of this scaffold towards various kinds of PPI targets.

The key point of this work is that very good ligand efficiency was achieved, whilst maintaining a relatively low average molecular weight of the compounds in the library. The typical molecular weight for drug candidates targeting PPIs is known to be $700\text{--}800 \text{ Da}$.¹⁸ This means that the compounds from this work can be considered as starting points for further optimization of the properties for targeting various kinds of PPIs. In other words, this library allows room for improvement.

Experimental

LCMS spectra were recorded on a Surveyor MSQ instrument (Thermo Fisher Scientific) using a Phenomenex Onyx Mono-lythic C18 $25 \times 4.6 \text{ mm}$ Part no.: CHO-7645 column and a gradient from 100% to 5% of mobile phase A (0.1% solution of formic acid in water) in mobile phase B (0.1% solution of formic acid in acetonitrile), with a flow rate of 1.5 mL min^{-1} . Detection was performed using two types of detectors: a PDA-photodiode array detector in the $200\text{--}800 \text{ nm}$ range, and atmospheric pressure chemical ionization (APCI) (+ or $-$ ions). The total run time was 4.5 min, and the injection volume was $2 \mu\text{L}$.

The ^1H and ^{13}C NMR spectra were recorded in CDCl_3 , using TMS as an internal standard, on a Varian Mercury console-400 NMR spectrometer, operated at 400 MHz for ^1H and 100 MHz for ^{13}C .

Table 1 Biological data for the compounds of general formula


The chemical structure shows a pyrazole ring with an N=N bond. The pyrazole ring is connected to two phenyl rings. The left phenyl ring has a substituent R3 at the para position. The right phenyl ring has substituents R1 at the para position and R4 at the ortho position. The pyrazole ring has a substituent R2 at the 4-position.

nn	R1	R2	R3	R4	MDM2/p53, IC ₅₀ (μM)	LE	Solubility (Ug ml ⁻¹)
1	2-OC ₃ H ₇	-C ₂ H ₄ Ph	2-OMe, 3-OMe	5-COOH	6.56	0.20	0.117
2	2-OCH ₂ CH(CH ₃) ₂	-C ₂ H ₄ Ph	2-OMe, 3-OMe	5-COOH	8.22	0.19	0.056
3	2-OEt	-C ₂ H ₄ Ph	2-OEt	5-COOH	10.65	0.21	0.022
4	2-OEt	-C ₂ H ₄ Ph	2-OMe, 3-OMe	5-COOH	13.98	0.20	>0.2
5	2-OC ₄ H ₉	-C ₂ H ₄ Ph	2-OMe, 3-OMe	5-COOH	14.15	0.19	0.066
6	2-OCH ₂ CH(CH ₃) ₂	-C ₂ H ₄ Ph	2-OEt	5-COOH	14.19	0.19	0.015
7	2-OC ₄ H ₉	-C ₂ H ₄ Ph	2-OEt	5-COOH	16.75	0.19	0.032
8	2-OMe	-CH ₂ Ph	4-F	5-C ₂ H ₄ COOH	16.98	0.21	0.066
9	2-OCH ₂ (3-Cl-Ph)	-CH ₂ Ph	2-OMe, 3-OMe	5-C ₂ H ₄ COOH	31.62	0.15	<0.015
10	2-OCH ₂ (3-Cl-Ph)	-C ₂ H ₄ Ph	2-OMe, 3-OMe	5-C ₂ H ₄ COOH	34.02	0.15	<0.015
11	2-OEt	-C ₂ H ₄ Ph	4-F	5-C ₂ H ₄ COOH	35.78	0.18	>0.2
12	2-OMe	-C ₂ H ₄ Ph	4-Cl	5-C ₂ H ₄ COOH	38.87	0.19	0.046
13	2-OCH ₂ (3-Cl-Ph)	-C ₂ H ₄ Ph	4-F	5-C ₂ H ₄ COOH	47.83	0.15	<0.015
14	2-OCH ₂ CH(CH ₃) ₂	-C ₂ H ₄ Ph	2-OEt	5-CH ₂ COOH	48.7	0.16	0.046
15	2-OCH ₂ (3-Cl-Ph)	-CH ₂ Ph	4-F	5-C ₂ H ₄ COOH	51.88	0.16	<0.015
16	2-OC ₄ H ₉	-C ₂ H ₄ Ph	2-OEt	5-CH ₂ COOH	54.06	0.16	0.096
17	2-OCH ₂ (3-Cl-Ph)	-CH ₂ Ph	2-OEt	5-CH ₂ COOH	54.39	0.15	<0.015
18	2-OC ₃ H ₇	-C ₂ H ₄ Ph	2-OMe, 3-OMe	5-CH ₂ COOH	60.6	0.16	0.117
19	2-OCH ₂ CH(CH ₃) ₂	-C ₂ H ₄ Ph	2-OMe, 3-OMe	5-CH ₂ COOH	68.32	0.15	0.056
20	2-OC ₃ H ₇	-CH ₂ Ph	2-OEt	5-COOH	68.75	0.17	0.096
21	2-OC ₃ H ₇	-C ₂ H ₄ Ph	2-OEt	5-CH ₂ COOH	71.98	0.16	0.066
22	2-OC ₃ H ₇	-CH ₂ Ph	2-OMe, 3-OMe	5-COOH	79.27	0.17	>0.2
23	2-OMe	-CH ₂ Ph	4-Cl	5-C ₂ H ₄ COOH	86.63	0.18	0.019
24	H	-C ₂ H ₄ Ph	2-OEt	4-COOH	91.22	0.18	>0.2
25	2-OEt	-CH ₂ Ph	4-F	5-C ₂ H ₄ COOH	100.8	0.17	<0.015
26	2-OEt	-C ₂ H ₄ Ph	2-OEt	5-CH ₂ COOH	102.4	0.16	>0.2
27	2-OEt	-C ₂ H ₄ Ph	2-OEt	5-C ₂ H ₄ COOH	105.4	0.16	0.102
28	2-OEt	-CH ₂ Ph	2-OEt	5-COOH	111.1	0.17	0.066
29	2-OC ₄ H ₉	-C ₂ H ₄ Ph	2-OMe, 3-OMe	5-CH ₂ COOH	115.6	0.15	0.117
30	2-OC ₄ H ₉	-CH ₂ Ph	2-OMe, 3-OMe	5-CH ₂ COOH	117.7	0.15	>0.2
31	2-OCH ₂ CH(CH ₃) ₂	-CH ₂ Ph	2-OMe, 3-OMe	5-CH ₂ COOH	120.0	0.15	>0.2
32	H	-C ₂ H ₄ Ph	4-F	4-COOH	127.9	0.2	0.096
33	2-OCH ₂ (2-Cl-Ph)	-CH ₂ Ph	4-F	5-CH ₂ COOH	129.8	0.14	<0.015
34	2-OMe	-C ₂ H ₄ Ph	2-OMe, 3-OMe	5-COOH	185.6	0.15	>0.2
35	2-OMe	-C ₂ H ₄ Ph	2-OEt	5-COOH	232.5	0.16	>0.2
36	2-OMe	-CH ₂ Ph	2-OEt	5-COOH	238	0.16	0.039
37	2-OCH ₂ (3-Cl-Ph)	-C ₂ H ₄ Ph	2-OEt	5-CH ₂ COOH	248.8	0.12	<0.015
38	2-OMe	-C ₂ H ₄ Ph	2-OEt	5-C ₂ H ₄ COOH	258.4	0.14	>0.2
39	2-OMe	-CH ₂ Ph	2-OEt	5-CH ₂ COOH	287.6	0.15	0.138
40	2-OEt	-CH ₂ Ph	2-OMe, 3-OMe	5-COOH	294.5	0.15	0.138
41	2-OC ₃ H ₇	-CH ₂ Ph	2-OMe, 3-OMe	5-CH ₂ COOH	328.6	0.14	>0.2
42	2-OMe	-C ₂ H ₄ Ph	2-OEt	5-CH ₂ COOH	339.2	0.14	>0.2
43	H	-CH ₂ Ph	2-OEt	4-COOH	346.4	0.16	0.117
44	2-OEt	-CH ₂ Ph	2-OMe, 3-OMe	5-CH ₂ COOH	348.2	0.14	>0.2
45	2-OEt	-CH ₂ Ph	2-OMe, 3-OMe	5-C ₂ H ₄ COOH	352.7	0.14	>0.2
46	2-OMe	-CH ₂ Ph	2-OEt	5-C ₂ H ₄ COOH	388.1	0.14	>0.2
47	2-OMe	-C ₂ H ₄ Ph	2-OMe, 3-OMe	5-C ₂ H ₄ COOH	436.5	0.13	>0.2
48	2-OMe	-CH ₂ Ph	2-OMe, 3-OMe	5-C ₂ H ₄ COOH	449.2	0.14	0.169
49	2-OMe	-CH ₂ Ph	4-F	5-CH ₂ COOH	594.7	0.15	>0.2
50	2-OMe	-C ₂ H ₄ Ph	2-OMe, 3-OMe	5-CH ₂ COOH	726.8	0.13	>0.2
51	2-OMe	-CH ₂ Ph	2-OMe, 3-OMe	5-CH ₂ COOH	967.3	0.13	>0.2
52	2-OMe	-CH ₂ Ph	2-OMe, 3-OMe	5-COOH	1018.0	0.13	>0.2
Nutlin-3					0.474	0.22	

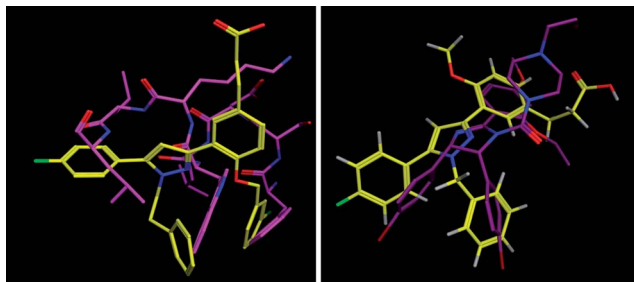


Fig. 3 Docking of compounds **8** and **13** into the MDM2 p53 binding site. Left pane: compound **13** was docked into the p53 binding site of PDB entry 1ycr. Compound **13** (yellow) and the transactivation domain of p53 from this entry (purple) are shown. Right pane: compound **8** was docked into the same complex as in the left pane. MDM2, with **8** docked into it, was then superposed onto the MDM2 complex with nutlin-2 (PDB entry 1rv1). Compound **8** (yellow) and nutlin-2 (purple) are shown.

The compounds were purified by HPLC on an Agilent 1200 HPLC Instrument. Experimental conditions: column: Luna® 5 µm C18(2) Axia packed (50 × 21.2 mm), mobile phase: A = 0.1% HCOOH in water, B = 0.1% HCOOH in acetonitrile, gradient: 1 minute at 98 : 2 (A/B), to 25 : 75 (A/B) over 8 minutes, flow rate: 60 mL min⁻¹, detection: UV at 270 nm, injection volume: 400 µL.

Methanol 99.8% (Aldrich) was used as a solvent for the scaffold synthesis and acetonitrile LC-MS Chromasolv (Fluka) was used for HPLC purification. The aldehydes were prepared *via* alkylation of methyl 3-formyl-4-hydroxybenzoate (Aldrich, CAS 24589-99-9) using the corresponding alkyl chlorides or alkyl bromides and potassium carbonate base in DMF. All of the nitrostyrenes, benzylhydrazine hydrochloride and phenethylhydrazine were purchased from Aldrich.

3-(5-(2,3-Dimethoxyphenyl)-1-phenethyl-1H-pyrazol-3-yl)-4-propoxybenzoic acid (**1**)

Phenethylhydrazine hydrochloride (MW 136, 34 mg, 0.25 mmol, 1 eq.) in methanol (0.6 ml) was added to a solution of methyl 3-formyl-4-propoxybenzoate (MW 222, 56 mg, 0.25 mmol, 1 eq.) in methanol (0.6 mL). After stirring at room temperature for 1 h, 2,3-dimethoxynitrostyrene (MW 209, 47 mg, 0.225 mmol, 0.90 eq.) was added in methanol (0.6 mL), and the reaction solution was stirred at room temperature, open to air, for 24 h. To hydrolyze the methyl ester to the corresponding benzoic acid, 0.2 mL of 20% NaOH solution was added and the reaction mixture was refluxed for 1 h. After acidifying to pH 7, the resulting mixture was concentrated and purified by HPLC to give a white solid (40 mg, 37% for the two steps). m.p. 86 °C, ¹H NMR δ (CDCl₃), ppm: 1.00 (3H, t, *J* = 7 Hz); 1.90 (2H, m); 3.20 (2H, t, *J* = 7 Hz); 3.62 (3H, s); 3.92 (3H, s); 4.12 (2H, t, *J* = 7 Hz); 4.35 (2H, t, *J* = 7 Hz); 6.62 (1H, dd, *J* = 8.5 Hz/3 Hz); 6.80 (1H, s); 7.00 (5H, m); 7.15 (3H, m); 8.12 (1H, dd, *J* = 8.5 Hz/3 Hz); 8.90 (1H, d, *J* = 3 Hz). ¹³C NMR δ (CDCl₃), ppm: 170.35; 160.36; 153.04; 147.30; 146.56; 140.21; 138.74; 131.30; 131.10; 129.94; 128.33; 126.27; 125.48; 123.90; 123.50; 122.76; 122.24; 113.40; 111.73; 108.20; 70.37; 60.73; 56.10; 51.28; 36.75; 22.64; 10.70. LC-MS *m/z*: 487 (M + H⁺), purity: 95%.

3-(5-(2,3-Dimethoxyphenyl)-1-phenethyl-1H-pyrazol-3-yl)-4-isobutoxybenzoic acid (**2**)

3-(5-(2,3-Dimethoxyphenyl)-1-phenethyl-1H-pyrazol-3-yl)-4-isobutoxybenzoic acid (**2**) was synthesized as described for **1** using phenethylhydrazine hydrochloride (MW 136, 34 mg, 0.25 mmol, 1 eq.), methyl 3-formyl-4-isobutoxybenzoate (MW 236, 59 mg, 0.25 mmol, 1 eq.) and 2,3-dimethoxynitrostyrene (MW 209, 47 mg, 0.225 mmol, 0.90 eq.) as the starting materials. The yield was 60 mg, 53% for the two steps. m.p. 87 °C, ¹H NMR δ (CDCl₃), ppm: 1.01 (6H, d, *J* = 7 Hz); 2.25 (1H, m); 3.20 (2H, t, *J* = 7 Hz); 3.62 (3H, s); 3.92 (5H, m); 4.35 (2H, t, *J* = 7 Hz); 6.60 (1H, dd, *J* = 8.5 Hz/3 Hz); 6.80 (1H, s); 7.00 (5H, m); 7.15 (3H, m); 8.00 (1H, dd, *J* = 8.5 Hz/3 Hz); 8.90 (1H, d, *J* = 3 Hz). ¹³C NMR δ (CDCl₃), ppm: 170.22; 160.47; 153.03; 147.26; 146.61; 140.24; 138.75; 131.43; 131.14; 128.93; 128.33; 126.23; 125.48; 123.91; 123.50; 122.83; 122.14; 113.39; 111.69; 108.21; 75.32; 60.71; 56.10; 51.29; 36.37; 28.42; 19.42. LC-MS *m/z*: 501 (M + H⁺), purity: 95%.

3-(5-(2,3-Dimethoxyphenyl)-1-phenethyl-1H-pyrazol-3-yl)-4-ethoxybenzoic acid (**4**)

3-(5-(2,3-Dimethoxyphenyl)-1-phenethyl-1H-pyrazol-3-yl)-4-ethoxybenzoic acid (**4**) was synthesized as described for **1** using phenethylhydrazine hydrochloride (MW 136, 34 mg, 0.25 mmol, 1 eq.), methyl 3-formyl-4-ethoxybenzoate (MW 208, 52 mg, 0.25 mmol, 1 eq.) and 2,3-dimethoxynitrostyrene (MW 209, 47 mg, 0.225 mmol, 0.90 eq.) as the starting materials. The yield was 50 mg, 47% for the two steps. m.p. 172 °C, ¹H NMR δ (CDCl₃), ppm: 1.50 (3H, t, *J* = 7 Hz); 3.20 (2H, t, *J* = 7 Hz); 3.65 (3H, s); 3.92 (3H, s); 4.25 (2H, q, *J* = 7 Hz); 4.35 (2H, t, *J* = 7 Hz); 6.62 (2H, dd, *J* = 8.5 Hz/3 Hz); 6.80 (1H, s); 7.00 (5H, m); 7.15 (3H, m); 8.15 (1H, dd, *J* = 8.5 Hz/3 Hz); 8.98 (1H, d, *J* = 3 Hz). ¹³C NMR δ (CDCl₃), ppm: 170.31; 160.21; 153.06; 147.32; 146.50; 140.19; 138.74; 131.25; 131.08; 128.94; 128.34; 126.24; 125.48; 123.89; 123.50; 122.74; 122.28; 113.42; 111.79; 108.23; 64.35; 60.76; 56.10; 51.28; 36.75; 14.79. LC-MS *m/z*: 473 (M + H⁺), purity: 95%.

3-(5-(2,3-Dimethoxyphenyl)-1-phenethyl-1H-pyrazol-3-yl)-4-butoxybenzoic acid (**5**)

3-(5-(2,3-Dimethoxyphenyl)-1-phenethyl-1H-pyrazol-3-yl)-4-butoxybenzoic acid (**5**) was synthesized as described for **1** using phenethylhydrazine hydrochloride (MW 136, 34 mg, 0.25 mmol, 1 eq.), methyl 3-formyl-4-butoxybenzoate (MW 236, 59 mg, 0.25 mmol, 1 eq.) and 2,3-dimethoxynitrostyrene (MW 209, 47 mg, 0.225 mmol, 0.90 eq.) as the starting materials. The yield was 47 mg, 42% for the two steps. m.p. 140 °C, ¹H NMR δ (CDCl₃), ppm: 0.95 (3H, t, *J* = 7 Hz); 1.50 (2H, m); 1.85 (2H, m); 3.20 (2H, t, *J* = 7 Hz); 3.62 (3H, s); 3.95 (3H, s); 4.13 (2H, t, *J* = 7 Hz); 4.35 (2H, t, *J* = 7 Hz); 6.65 (1H, dd, *J* = 8.5 Hz/3 Hz); 6.80 (1H, s); 7.00 (5H, m); 7.15 (3H, m); 8.12 (1H, dd, *J* = 8.5 Hz/3 Hz); 8.98 (1H, d, *J* = 3 Hz). ¹³C NMR δ (CDCl₃), ppm: 170.19; 160.38; 153.04; 147.30; 146.55; 140.22; 138.75; 131.31; 131.10; 128.93; 128.33; 126.23; 125.50; 123.90; 123.51; 122.79; 122.16; 113.42; 111.72; 108.19; 64.48; 60.72; 56.11; 51.29; 36.74; 31.31; 19.35; 13.73. LC-MS *m/z*: 501 (M + H⁺), purity: 95%.

3-(5-(2-Ethoxyphenyl)-1-phenethyl-1H-pyrazol-3-yl)-4-isobutoxybenzoic acid (6)

3-(5-(2-Ethoxyphenyl)-1-phenethyl-1H-pyrazol-3-yl)-4-isobutoxybenzoic acid (6) was synthesized as described for **1** using phenethylhydrazine hydrochloride (MW 136, 34 mg, 0.25 mmol, 1 eq.), methyl 3-formyl-4-isobutoxybenzoate (MW 236, 59 mg, 0.25 mmol, 1 eq.) and 2-ethoxynitrostyrene (MW 193, 44 mg, 0.225 mmol, 0.90 eq.) as the starting materials. The yield was 59 mg, 54% for the two steps. m.p. 205 °C, ^1H NMR δ (CDCl_3), ppm: 1.00 (6H, d, $J = 7$ Hz); 1.30 (3H, t, $J = 7$ Hz); 2.20 (1H, m); 3.20 (2H, t, $J = 7$ Hz); 3.92 (2H, d, $J = 7$ Hz); 4.05 (2H, q, $J = 7$ Hz); 4.35 (2H, t, $J = 7$ Hz); 6.75 (1H, s); 7.00 (6H, m); 7.15 (3H, m); 7.37 (1H, t, $J = 8.5$ Hz); 8.12 (1H, d, $J = 8.5$ Hz); 8.80 (1H, d, 3 Hz). ^{13}C NMR δ (CDCl_3), ppm: 170.06; 160.44; 156.46; 146.57; 140.96; 138.81; 131.95; 131.39; 131.03; 130.19; 128.86; 128.34; 126.22; 122.83; 122.28; 120.65; 120.61; 112.64; 111.72; 108.28; 75.34; 64.27; 51.20; 36.87; 28.41; 19.45; 14.77. LC-MS m/z : 485 ($\text{M} + \text{H}^+$), purity: 95%.

3-(5-(2-Ethoxyphenyl)-1-phenethyl-1H-pyrazol-3-yl)-4-butoxybenzoic acid (7)

3-(5-(2-Ethoxyphenyl)-1-phenethyl-1H-pyrazol-3-yl)-4-butoxybenzoic acid (7) was synthesized as described for **1** using phenethylhydrazine hydrochloride (MW 136, 34 mg, 0.25 mmol, 1 eq.), methyl 3-formyl-4-butoxybenzoate (MW 236, 59 mg, 0.25 mmol, 1 eq.) and 2-ethoxynitrostyrene (MW 193, 44 mg, 0.225 mmol, 0.90 eq.) as the starting materials. The yield was 49 mg, 45% for the two steps. m.p. 184 °C, ^1H NMR δ (CDCl_3), ppm: 0.98 (3H, t, $J = 7$ Hz); 1.35 (3H, t, $J = 7$ Hz); 1.55 (2H, m); 1.88 (2H, m); 3.15 (2H, t, $J = 7$ Hz); 4.05 (2H, q, $J = 7$ Hz); 4.15 (2H, t, $J = 7$ Hz); 4.35 (2H, t, $J = 7$ Hz); 6.75 (1H, s); 7.00 (6H, m); 7.18 (3H, m); 7.40 (1H, t, $J = 8.5$ Hz); 8.10 (1H, dd, $J = 8.5$ Hz/3 Hz); 8.98 (1H, d, $J = 3$ Hz). ^{13}C NMR δ (CDCl_3), ppm: 169.98; 160.35; 156.45; 146.52; 140.96; 138.81; 131.97; 131.28; 130.99; 130.20; 128.86; 128.35; 126.22; 122.81; 122.25; 120.64; 120.60; 112.61; 111.75; 108.26; 68.51; 64.26; 51.22; 36.86; 31.31; 19.35; 14.79; 13.75. LC-MS m/z : 485 ($\text{M} + \text{H}^+$), purity: 93%.

Data for the LC-MS, yields and purities of the other compounds are given in the ESI.†

Biological testing

The test compounds in DMSO were diluted in Assay Buffer (10 mM PBS, pH 7.4, 2 mM DTT, 0.1 mg mL^{-1} BGG, 0.01% Triton X-100). An aliquot was transferred into 96-well polypropylene microplates (Corning, 3915) and mixed with 0.2 μM (final concentration) of 6His-MDM2 (amino acids 1–118, in house). The samples were incubated at room temperature (RT) for 10 min, and then 10 nM (final concentration) of FITC-p53 (amino acids 17–26) (Anaspec, 62386) was added. The samples were incubated at RT for 30 min and FP (fluorescence polarization) was read on a TECAN Infinite F500 instrument (Ex485/Em535).

Molecular docking

The crystal structure of the MDM2 complex with p53 was obtained from the RCSB protein data bank. Compounds **8** and

13 were docked into the binding site of MDM2 using the MOE docking module with the London dG scoring function.¹⁹ The binding site was determined as the residues of MDM2 at the nearest distance (within 4.5 Å) to the p53 residues from Phe19 to Leu26. To further guarantee the appropriate scoring, the additional pharmacophore constraint was generated; one hydrophobic center of each docked compound should be positioned in the Trp23-binding region of MDM2. The best scoring conformations were chosen for each compound.

Conclusions

A new class of alpha-helix mimetics, based on the phenyl-pyrazole-phenyl (6-5-6) system, was designed and synthesized. The ability of the new compounds to inhibit PPIs was exemplified in the MDM2-p53 binding assay. The library revealed an excellent hit rate of 15%, has satisfactory physico-chemical properties (~38% soluble compounds), and the ligand efficiency of the best compound was found to be 0.21 (compared to 0.22 for nutlin-3 in the same assay). A dual mode of action of these inhibitors was suggested based on computer modeling: depending on the nature of the substituents they could act as either alpha-helix backbone mimetics or alpha-helix binding epitope mimetics.

A new feasible one-pot synthetic strategy comprising the regioselective synthesis of substituted pyrazoles was applied and adopted for the library synthesis. Bearing in mind the rather small molecular weights of the new compounds, in terms of PPI inhibitor properties they can be considered as starting points for further optimization of the properties towards improving their activity and selectivity against various types of PPIs.

Acknowledgements

We thank Dr Vitaly Skosyrev for his help in performing the biological experiments.

References

- 1 D. C. Fry, *Curr. Protein Pept. Sci.*, 2008, **9**, 240–247.
- 2 V. Azzarito, K. Long, N. S. Murphy and A. J. Wilson, *Nat. Chem.*, 2013, **5**, 161–173.
- 3 H. Yin, G.-I. Lee and A. D. Hamilton, in *Drug Discovery Research: New Frontiers in the Post-Genomic Era*, ed. Z. Huang, John Wiley & Sons, Inc, 2007, pp. 280–298.
- 4 L. Chen, H. Yin, B. Farooqi, S. Sebt, A. D. Hamilton and J. Chen, *Mol. Cancer Ther.*, 2005, **4**(6), 1019–1025.
- 5 L. T. Vassilev, B. T. Vu, B. Graves, D. Carvajal, F. Podlaski, Z. Filipovic, N. Kong, U. Kammlott, C. Lukacs, C. Klein, N. Fotouhi and E. A. Liu, *Science*, 2004, **303**, 844–848.
- 6 I. Saraogi and A. D. Hamilton, *Biochem. Soc. Trans.*, 2008, **36**, 1414–1417.
- 7 B. N. Bullock, A. L. Jochim and P. S. Arora, *J. Am. Chem. Soc.*, 2011, **133**, 14220–14223.
- 8 D. Fry, K. S. Huang, P. D. Lello, P. Mohr, K. Muller, S. S. So, T. Harada, M. Stahl, B. Vu and H. Mauser, *ChemMedChem*, 2013, **8**(5), 726–732.

- 9 C. P. Gomes, A. Metz, J. W. Bats, H. Gohlke and M. W. Gobel, *Eur. J. Org. Chem.*, 2012, 3279–3277.
- 10 I. Ehlers, P. Maity, J. Aubé and B. König, *Eur. J. Org. Chem.*, 2011, 2474–2490.
- 11 A. P. Higuieruelo, A. Schreyer, G. R. J. Bickerton, W. R. Pitt, C. R. Groom and T. L. Blundell, *Chem. Biol. Drug Des.*, 2009, 74, 457–460.
- 12 X. Deng and N. S. Mani, *J. Org. Chem.*, 2008, 73, 2412–2415.
- 13 X. Deng and N. S. Mani, *Org. Lett.*, 2006, 8(16), 3505–3508.
- 14 C. Reynes, H. Host, A.-C. Camproux, G. Laconde, F. Leroux, A. Mazars, B. Deprez, R. Fahraeus, B. O. Villoutreix and O. Sperandio, *PLoS Comput. Biol.*, 2010, 6(3), 1–15.
- 15 O. Sperandio, C. H. Reynes, A.-C. Camproux and B. O. Villoutreix, *Drug Discovery Today*, 2010, 15, 220–229.
- 16 A. Neugebauer, R. W. Hartmann and C. D. Klein, *J. Med. Chem.*, 2007, 50, 4665–4668.
- 17 O. Schon, A. Friedler, M. Bycroft, S. M. V. Freund and A. R. Fersht, *J. Mol. Biol.*, 2002, 323, 491–501.
- 18 D. C. Fry, C. Wartchow, B. Graves, C. Janson, C. Lukacs, U. Kammlott, C. Belunis, S. Palme, C. Klein and B. Vu, *ACS Med. Chem. Lett.*, 2013, 4, 660–665.
- 19 Molecular Operating Environment (MOE), Chemical Computing Group Inc., 1010 Sherbrooke Street West, Suite 91, Montreal, H3A 2R7, Canada.